CrystEngComm

Accepted Manuscript

This is an *Accepted Manuscript*, which has been through the Royal Society of Chemistry peer review process and has been accepted for publication.

Accepted Manuscripts are published online shortly after acceptance, before technical editing, formatting and proof reading. Using this free service, authors can make their results available to the community, in citable form, before we publish the edited article. We will replace this *Accepted Manuscript* with the edited and formatted *Advance Article* as soon as it is available.

You can find more information about *Accepted Manuscripts* in the Information for Authors.

Please note that technical editing may introduce minor changes to the text and/or graphics, which may alter content. The journal's standard Terms & Conditions and the Ethical guidelines still apply. In no event shall the Royal Society of Chemistry be held responsible for any errors or omissions in this *Accepted Manuscript* or any consequences arising from the use of any information it contains.

ROYAL SOCIETY OF CHEMISTRY

www.rsc.org/crystengcomm

Cite this: DOI: 10.1039/c0xx00000x

www.rsc.org/xxxxxx

ARTICLE TYPE

3D hierarchical ZnOHF nanostructures: synthesis, characterization and photocatalytic properties

Miao Wang*, Tongming Sun, Yujun Shi, Guoqing Jiang and Yanfeng Tang*

Received (in XXX, XXX) Xth XXXXXXXXX 20XX, Accepted Xth XXXXXXXXX 20XX

DOI: 10.1039/b000000x

Abstract: 3D hierarchical ZnOHF nanoflowers with mean diameter of 200 nm have been synthesized via a simple template-free hydrothermal route by using $(NH_4)_2SiF_6$ as the fluoride source. The crystalline phase and morphologies of the as-prepared products have been characterized by XRD, SEM and TEM. The XRD results show that the products are well-crystallized orthorhombic phase of ZnOHF. The SEM and TEM results indicate that the ZnOHF nanoflowers are assembled by numerous nanoflakes with mean thickness of 20 nm. Some factors influencing the morphologies of the ZnOHF nanostructures have been systematically investigated, such as the reaction time, temperature and fluoride source. A growth mechanism is proposed on the basis of a series of time-dependent morphological evolution results. The hierarchical ZnOHF nanoflowers exhibit a high specific surface area up to 97.1919 m^2/g with a pore size of 50.098 nm. The as-obtained ZnOHF can be transformed into ZnO nanoflowers by calcination in air at 600 °C. The photocatalytic properties of the ZnOHF have been studied by the decomposition of methyl orange (MO) under UV light irradiation. The results indicate that the flower-like ZnO nanostructures are chemically stable, and the efficiency remained almost the same after five times recycle.

Introduction

In recent years, 3D hierarchical architectures have received more and more research attentions for their distinctive physicochemical properties in comparison with conventional nanocrystallites. To date, lots of researches have devoted to exploring and fabricating functional materials with hierarchical architectures for achieving novel or enhanced properties. So far, various hierarchical structures have been prepared by the self-assembly of low-dimensional nanoscaled units.[1-5] Generally, the synthesis often relies on templated approaches by adding inorganics, organics, polymers or surfactants, which will bring high cost and tedious synthetic procedures. Thus, development of mild, template-free and one-step methods for hierarchically architectures are of great importance not only to the fundamental scientific interests but also potential technological applications.

ZnOHF, as an important zinc-containing material, has been widely used in the development of new functional materials such as selective oxidation catalysts, photoluminescence materials and optoelectronics devices.[6-10] Besides, it has been widely used as a precursor for the synthesis of ZnO nanostructures.[7-13] Furthermore, ZnOHF has been proved as an effective photocatalyst for decomposing organic compounds and organic dyes.[14-15] It is well known that the chemical or physical performance strongly depends on the morphology, dimension and surface area of nanomaterials. Recently, numerous efforts have been devoted to the exploration of ZnOHF micro/nanostructures. Nowadays, many synthetic routes have been employed to prepare the ZnOHF nano/microstructures including hydrothermal methods,[7, 14] solution-based method,[15] electrochemical route [8, 12-13] and microwave irradiation.[11, 16-17] Consequently, a series of ZnOHF nano/microstructures, such as nanorods,[8-9,12-13] net-like,[7] nanofibers,[15-16] nanobelts[17] and nanotubes of ZnOHF[14] have been successfully fabricated. Hierarchical ZnOHF architectures possess large surface area and more active sites, which are feasible to the better contact of the reactants with the surface of ZnOHF and transport of organic pollutants. Therefore, the fabrication of desired 3D hierarchical nanostructures is very important due to its peculiar structure and photocatalytic property. In this paper, we report the successful synthesis of hierarchical nanoflakes-assembled ZnOHF nanoflowers via a facile hydrothermal route by using $(NH_4)_2SiF_6$ as the fluoride source. However, to the best of our knowledge, there has been no report on the preparation of such ZnOHF nanocrystals. This method does not need any hard or soft template or surfactant, avoiding the procedures and cost for their removal in the product. The effects of synthesis parameters (fluoride source, reaction time and temperature) on the crystallinity and morphologies of the as-prepared products are investigated. Furthermore, the ZnOHF nanoflowers have excellent photocatalytic activity for the degradation of MO under UV light irradiation. The stability of the photocatalytic activity of the flower-like ZnOHF nanocrystals are evaluated by five recycling runs.

Experimental Section

2.1 Synthesis of 3D hierarchical flower-like ZnOHF nanostructures

All the chemicals including $ZnSO_4 \cdot 7H_2O$ and $(NH_4)_2SiF_6$ are A. R. grade. Particulate TiO_2 (P-25) is commercially available from Aladdin Reagents (China) Co., Ltd. Degussa P-25 TiO_2 was a mixture of 75% anatase and 25% rutile. In a typical process, 3.0 mmol $ZnSO_4 \cdot 7H_2O$ and 0.5 mmol $(NH_4)_2SiF_6$ were dissolved in 25 mL distilled water and the mixture was stirred at

CrystEngComm Accepted Manuscript

room temperature for 10 min. Then the mixed solution was transferred into a 30 mL Teflon-lined autoclave. After being sealed and heated at 120 ℃ for 12 h, the autoclave was gradually cooled to room temperature. The resulting white products were precipitated by centrifugation, washed with distilled water and ethanol and finally dried under vacuum at 70 ℃ for 3h. For a comparative study, the experiments with different temperature and reaction time were also conducted under similar conditions, respectively.

2.2 Characterization

X-ray diffraction (XRD) patterns were recorded on a Bruker AXSD8 ADVANCE X-ray diffractometer (Cu Kα radiation λ = 0.15418 nm) at room temperature. The operation voltage and current were maintained at 40 kV and 40 mA, respectively. The morphologies and microstructures of the as-synthesized samples were studied by scanning electron microscopy (SEM, Hitachi S-4800) employing an operating voltage of 15 kV and transmission electron microscopy (TEM, JEOL 2100) with a 200 kV accelerating voltage. Nitrogen adsorption-desorption isotherms were collected using a Micromeritics ASAP2020C apparatus at 77 K. The pore size distribution plots were obtained by the Barret-Joyner-Halenda (BJH) model. The thermogravimetric analysis was performed on PerkinElmer-DTA7.

2.3 Measurement of photocatalytic activity

The photodegradation experiments were performed in a slurry reactor containing 50 mL of a 20 mg L^{-1} solution of MO and 30 mg of catalyst. A 250 W high-pressure mercury lamp with a maximum emission at approximately 365 nm was used as the UV source. An electric fan and cycled condensate water were used to prevent thermal catalytic effects. Prior to irradiation, the suspension was kept in the dark under stirring for 30 min to ensure the establishing of an adsorption/desorption equilibrium. During irradiation, 3.5 mL of the suspension was taken out at given time intervals. After irradiation with UV light, the suspensions were centrifuged to remove the particles. The UV–vis absorption spectra were obtained on a Shimadzu UV-2401PC spectrophotometer.

Results and discussion

XRD was used to characterize the crystalline phase and purity of the samples. Fig. 1 shows the XRD patterns of the as-prepared ZnOHF samples for the time-dependent experiments. The influence of reaction time on the crystalline phase was demonstrated through the changes of XRD patterns. As shown in Fig. 1a, all diffraction peaks of the samples prepared in the typical procedure are perfectly indexed to the orthorhombic phase of ZnOHF, which are in agreement with the literature value (JCPDS file No.74-1816). No peaks of impurities are observed. The strong and narrow diffraction peaks indicate that the samples are well crystallized. While other reaction conditions were kept identical, the XRD patterns of the products obtained from 6 h to 0.5 h are shown in Fig. 1b-e. The diffraction peaks can also be indexed as orthorhombic phase of ZnOHF, indicating that reaction time has no obvious effects on the crystalline phase of the products. However, the XRD pattern of the samples obtained within 12 h shows higher diffraction peaks than those of obtained from 3 h, which reveals the improved crystalline of the product with prolonging the reaction time.

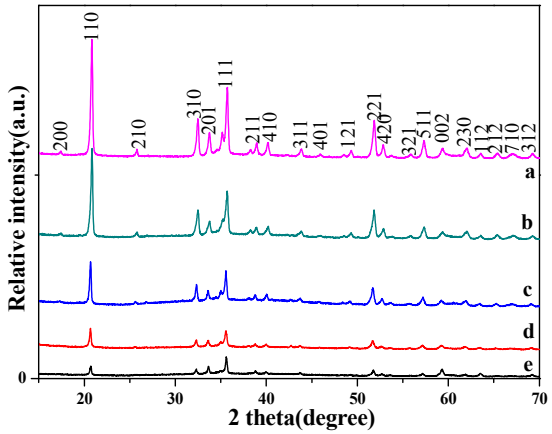

Fig. 1 XRD patterns of the ZnOHF samples obtained at different reaction times: (a) 12h; (b) 6h; (c) 3 h; (d) 1 h; (e) 0.5 h.

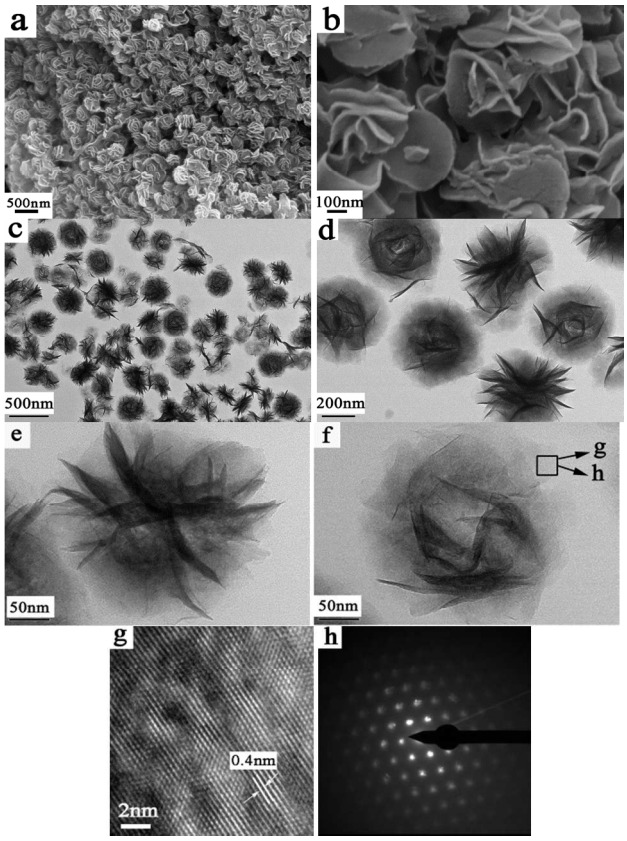

Fig 2. SEM (a-b), TEM (c-f), HRTEM (g) images and SAED pattern (h) of the ZnOHF nanoflowers obtained in the typical process.

The sizes and morphologies of the as-prepared products were characterized by SEM and TEM. Fig. 2a is typical low-magnification SEM images of the as-prepared product, from which numerous 3D hierarchical flower-like ZnOHF nanostructures with diameter of 200-300 nm can be clearly observed. No other morphologies can be detected, indicating a

CrystEngComm Accepted Manuscript

This journal is © The Royal Society of Chemistry [year]

high yield of these nanoflowers. A magnified SEM image (Fig. 2b) reveals the interesting fact that the ZnOHF flower-like structures are assembled by many interweaving and slightly bending nanoflakes with a thickness of 20 nm. The structures of the hierarchical flower-like ZnOHF were further investigated by TEM. As shown in Fig. 2c, the samples are composed of uniform flower-like particles with diameters that range from 200 to 300 nm. The hierarchical architecture consists of many randomly arranged thin nanoflakes like petals grown from the center of the flower (Fig. 2d-e), which is in accordance with the SEM images. Impressively, some nanoflowers appear spherical because they do not lie tightly on the TEM grid (Fig. 2f). A representative HRTEM image at the edge of an individual ZnOHF nanoflake from a single nanoflower (marked in Fig. 2f) was shown in Fig. 2g. The lattice fringes are clearly visible with a spacing of 0.4 nm, which agrees well with the lattice spacing of (110) crystal planes. The SAED pattern (Fig. 2h) recorded on the same part of the nanoflake proves the single-crystalline nature, which further supports the claim of crystallinity for ZnOHF nanoflowers. As much as we concerned, little work has been conducted on the hierarchical flower-like ZnOHF nanostructures assembled by nanoflakes.

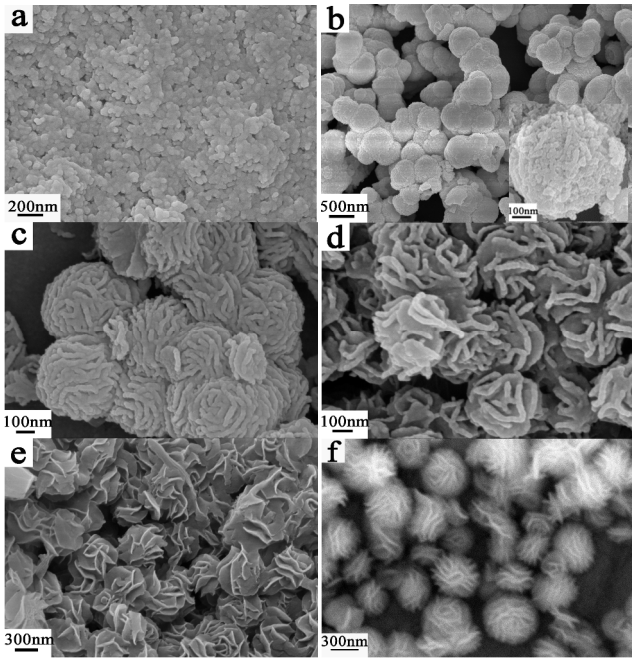

Fig. 3 SEM images of the ZnOHF samples prepared from different reaction time: (a) 10min; (b) 0.5 h; (c) 1h; (d) 3 h; (e) 6 h and (f) 24 h.

To get an insight into the formation of hierarchical flower-like ZnOHF nanostructures, controlled experiments were performed to investigate the effects of reaction parameters. Time-dependent experiments were carried out and the intermediate products were inspected by SEM. It is found that the reaction time has great effect on the final morphologies of the product. Fig. 3a-f represent the FE-SEM images of the precursor intermediates obtained at different reaction periods of 10 min (a), 0.5 h (b), 1 h (c), 3 h (d) , 6 h (e) and 24 h (f), respectively. As shown in Fig. 3a, the product is composed of many aggregated tiny nanoparticles within 10 min. At the stage of 0.5 h, there are abundant aggregated sub-microspheres with diameters about 300-400 nm (Fig. 3b). The SEM image (inset Fig. 3b) from a single sphere indicates that it is constructed from many tiny irregular nanoparticles. When the reaction time is prolonged to 1 h, the SEM image (Fig. 3c) shows that many spherical agglomerates are formed. It is noted that the surface are covered with small strip-like protuberances. Interestingly, this shape is similar to the human brain. With increase of the reaction time to 3 h, the protuberances grow into nanoslices. Thus, the surface of the architecture is much clearer. Further extending the reaction time to 6 h, some 3D hierarchical flower-like nanospheres are formed, and the nanospheres are composed of lots of intersected nanoflakes. After reaction for 24 h, it can be seen that the products still remain in the porous flower-shaped morphology, but the average grain size increases to 500-600 nm (Fig. 3f). Therefore, the images in Fig. 3a-f can clearly demonstrate the shape evolution of the obtained products from nanoparticles to nanoflowers.

The pH values of the solution were measured systematically. In a typical procedure, the pH values of the initial and final aqueous solution are 6.38 and 4.35, respectively. The pH values of the initial and final reaction are found to be varied from 6.38 to 6.14 (1 h), 5.78 (3 h) and 4.97 (6 h), respectively. These results reveal that there is an increase of the acidity of the reaction mixture after hydrothermal reaction.

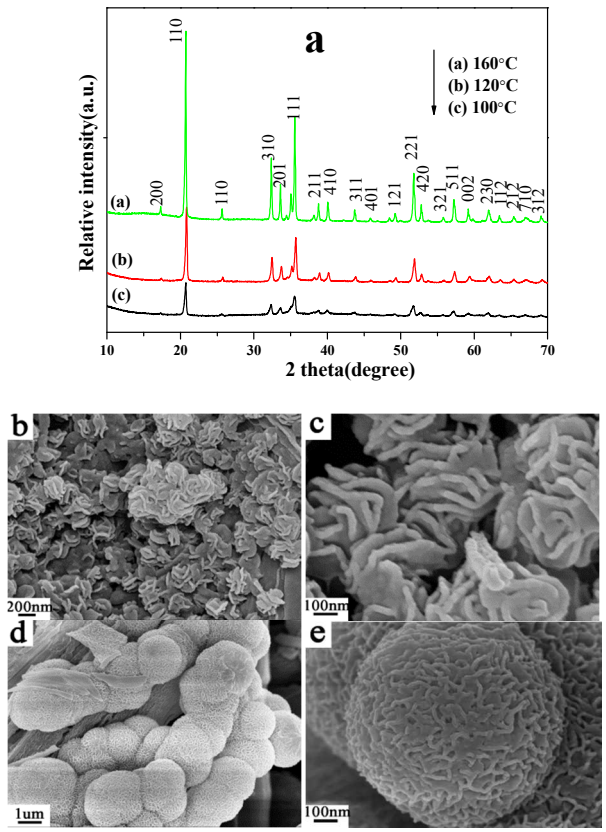

Fig. 4 XRD patterns (a) and SEM images of the ZnOHF samples prepared from different temperature: (b-c) 100 °C and (d-e) 160 °C within 12 h.

The effects of reaction temperature on the morphology and crystalline phase of products were studied. Fig. 4a shows the XRD patterns of the products obtained from different temperature within 12 h. All of the diffraction peaks can be indexed to

CrystEngComm Accepted Manuscript

orthorhombic phase of ZnOHF by comparison with the data from JCPDS file No.74-1816. The diffraction peaks of the products prepared at 160 °C are much sharper than those of 120 °C and 100 °C, revealing the improved crystalline after increasing the reaction temperature. Herein, to meet the requirements of homogeneous nucleation, the reaction was carried out at a moderate temperature (120 °C). Fig. 4b-e show the SEM images of the ZnOHF obtained at different hydrothermal temperature. When the temperature is fixed as 100 °C, many irregular aggregated flower-like nanostructures are obtained (Fig. 4b). The magnified SEM image (Fig. 4c) reveals that the flower-like nanostructures are composed of tiny nanoslices, which is similar to the case of 120 °C in a period of 3 h. When the reaction temperature is increased to 160 °C, as shown in Fig. 4d, there are many aggregated uniform spheres with diameter of 1-1.5 μm. The ZnOHF microsphere exhibits a hierarchical porous structure and the surface of the sphere consists of incompact arranged nanoflakes (Fig. 4e). Therefore, the temperature has a remarkable effect on the morphology of ZnOHF micro/nanostructures.

As well known, hydrothermal or solvothermal routes can not only induce the formation of well crystallized products at low temperatures, but also can control the phase, shape and size of the resultant products simply through adjusting the synthesis conditions such as temperature, pH, etc. In the present study, the precursor was treated with $(NH_4)_2SiF_6$ aqueous solution at different temperatures in the absence of surfactant-assistant and microemulsion or any other additives, thus, counterion effects on the formation of hierarchical flower-like ZnOHF nanostructures should not be neglected. The anionic counterions could selectively adsorb on the specific faces of the growing crystals and inhibit the crystal growth. Further increasing the temperature resulted in the formation of ZnOHF microspheres with rather rough surfaces (Fig. 4d-e). These observations show an increase in the anisotropy of the nanostructures with a lowering of temperature. In addition, driven by reducing the surface energy of nanoparticles, the products grow into ZnOHF microspheres. As a result, smaller particles are formed at lower temperature and the size increases as the hydrothermal temperature is increased. These results underline that the growth temperature has significant influence on the growth of ZnOHF micro/nanostructures. ZnOHF micro/nanostructures with different morphologies and different dimensions are prepared by controlling the nucleation and subsequent crystal growth process through tuning the reaction temperature.

For a comparative study, the experiments with different fluoride source (NH_4BF_4, $(NH_4)_2SiF_6$ and K_2SiF_6) were also investigated under similar conditions, respectively (Fig. S1, Supporting Information). In our previous work, NH_4BF_4 was used as fluoride source to synthesize ZnOHF nanotubes.[14] It is obvious that the morphology of ZnOHF can be controllably synthesized by varying the fluoride sources. For NH_4BF_4 and $(NH_4)_2SiF_6$, the positive ion in the two fluoride sources is the same, but the only difference is the negative central ion. Resultantly, hierarchical nanotubes-assembled microstructures and nanoflakes-assembled nanoflowers were prepared, respectively. Therefore, it is believed that the negative ions are responsible for the different morphologies of the as-prepared ZnOHF. It is possible that the formed byproducts will absorb on the surface of the initially formed ZnOHF particles, which will control the final morphology of the as-prepared ZnOHF. In order to investigate the effect of fluoride source, another complex fluoride, K_2SiF_6 was used instead of $(NH_4)_2SiF_6$ to synthesize ZnOHF by an identical procedure. Consequently, similar hierarchical flower-like ZnOHF nanostructures were obtained. Therefore, it is assumed that the structures of the positive ion (K^+ and NH_4^+) in the fluoride sources have no great effect on the morphologies of the as-prepared ZnOHF. These results indicate that the use of SiF_6^{2-} as F^- source is indispensable for obtaining the hierarchical flower-like ZnOHF nanostructures.

$$SiF_6^{2-} + 3H_2O \rightarrow 2F^- + H_2SiO_3 + 4HF \quad (1)$$

$$Zn^{2+} + F^- \leftrightarrow ZnF^+ \quad (2)$$

$$ZnF^+ + OH^- \leftrightarrow ZnOHF \quad (3)$$

It is known that SiF_6^{2-} is slowly decomposed in the reaction mixture to produce F^- anions, and then F^- anions react with metal ions to form inorganic metal fluorides, which have been proven in previous work.[18-20] The hydrolysis process of SiF_6^{2-} is very slow to produce F^- anions, and this step will keep the F^- ions in the solution. In the current study, the F^- ions are first released from $(NH_4)_2SiF_6$ and then react with the Zn^{2+} ions to form ZnF^+ complexes. The ZnF^+ complexes will form in the presence of F^- under neutral or weak alkaline conditions, and consequently lead to the slow nucleation ZnOHF occurs during further hydrolysis.[21-22] Therefore, it can be assumed that $(NH_4)_2SiF_6$ molecule, not noly as fluoride source but also as a structure directing agent, facilitates the nucleation and growth of such unique structures along a certain growth direction. Herein, $(NH_4)_2SiF_6$ is hydrolyzed to produce F^- ions when the molar ratio of $(NH_4)_2SiF_6/Zn^{2+}$ was 0.5:3 and only ZnOHF precipitated as described by Eqs(1-3).

From the above experimental results and analysis, the possible formation mechanism of hierarchical flower-like ZnOHF nanostructures is proposed based on the time-dependent morphology evolution process, as shown in scheme 1. (***i***) Fast nucleation and nuclei growth. At the initial reaction stage, nanoparticles are obtained from the reaction between Zn^{2+} and SiF_6^{2-} under hydrothermal condition. Because the surface energy of nanoparticles is generally high, the new nucleuses in the solution prefer to aggregate each other to form microspheres that become the core of the flower-like structure. Thus, nanoparticles-aggregated sub-microspheres are formed. (***ii***) Dissolution-recrystallization growth. Once the ZnOHF microspheres are formed, the decomposed products from $(NH_4)_2SiF_6$ can selectively adsorbed onto certain crystallographic planes of the ZnOHF seeds. In the following stage, the particles oriented, agglomerated, and recrystallized on the surfaces of the spherical structures. Thus, ZnOHF nanoparticles tend to grow into protuberances aggregated spherical agglomerates. (***iii***) Further growth. The formed ZnF^+ complexes will spontaneously nucleate onto the small protuberances which can provide many high-energy sites for nanocrystalline growth. In a further crystallization process, as the growth rates of different crystal facets are unequal, some specific crystalline planes are preferential grew to some extent, thus, nanoflakes are formed. It can be observed that the surface of the nanoflake in the flower-

CrystEngComm Accepted Manuscript

This journal is © The Royal Society of Chemistry [year]

like structure is very smooth, probably due to the Ostwald ripening. With the reaction going on, driven by reducing the surface energy of nanoparticles, the products continuously grow into hierarchical nanoflakes-assembled flower-like ZnOHF nanostructures. The results reveal that reaction time is a main factor to form nanoflakes-based nanoflowers, that is, the Ostwald ripening process is indispensable. Actually, this model has already been demonstrated and proven to be feasible to fabricate hierarchical micro/nanostructures.[1,23-24]

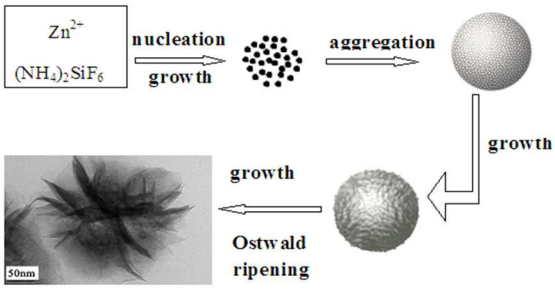

Scheme 1. Illustration of the growth process of hierarchical flower-like ZnOHF nanostructures.

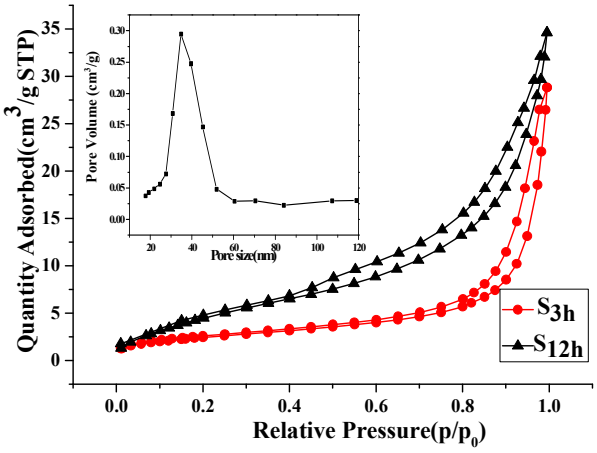

Fig. 5 Nitrogen adsorption-desorption isotherm and pore size distribution curves (inset) of the ZnOHF nanocrystals obtained from different reaction time.

Nitrogen adsorption-desorption isotherms were measured to determine the surface area and pore volume, and the corresponding results are presented in Fig. 5. The isotherm displays a typical IV isotherm of a type H3 hysteresis loop at relative pressure (P/P_0) between 0.4 and 1.0, suggesting the presence of mesopores in the products without a doubt. The BET surface of the hierarchical flower-like ZnOHF nanostructures (S_{12h}) is 97.1919 m^2/g. The pore size distribution is calculated from the desorption branch of the nitrogen isotherm by the BJH method, as shown in Fig. 5 inset. The results show that the average pore width of resultant hierarchical flower-like ZnOHF nanostructures is approximately 50.098 nm, and the pore volume is 0.2623 cm^3/g. The BET surface of the hierarchical flower-like ZnOHF nanostructures obtained from 3h (S_{3h}) is 73.2157 m^2/g,

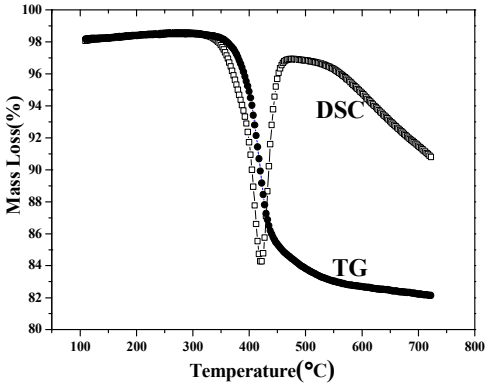

Fig. 6 TG and DSC profiles of the hierarchical flower-like ZnOHF nanostructures

ZnOHF was reported to be a precursor of ZnO.[7-13] The thermal behavior of ZnOHF was investigated by means of TG-DSC in N_2 atmosphere. The TG and DSC were performed from 50 °C to 800 °C at a heating rate of 10 °C /min and the profiles are shown in Fig. 6. There is an endothermic peak in the DSC curve due to the decomposition of ZnOHF. TG curve shows that 17.2% weight loss was observed in the temperature range from 350 ºC to 500 ºC due to the removal of small molecules HF, which is in agreement with the theoretical value of 17 % from ZnOHF to ZnO.

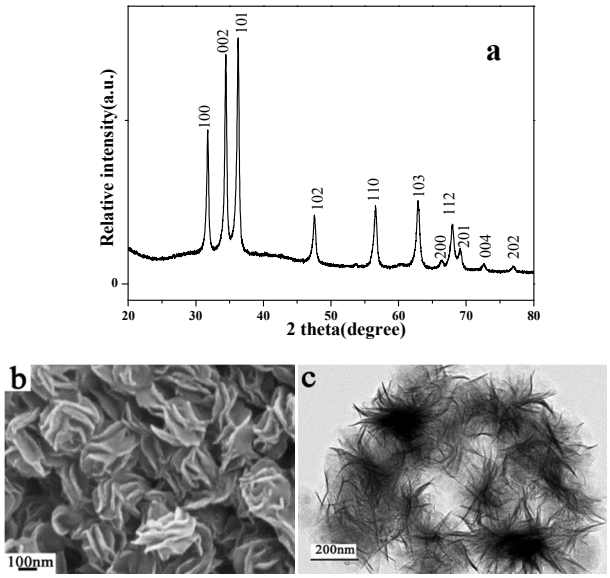

Fig. 7 XRD (a), SEM (b) and TEM (c) images of the as-prepared ZnO by calcining the precursor ZnOHF at 600 °C for 2h.

From the result of TG-DSC, the as-synthesized ZnOHF were calcinated in air at 600 °C for 2 h. The XRD pattern of the product is shown in Fig. 7a. All the diffraction peaks can be indexed to a hexagonal phase of ZnO (JCPDS file No.80- 0075), suggesting that the precursor ZnOHF has been transformed into ZnO by calcination at 600 °C. The SEM and TEM images of the as-synthesized ZnO are shown in Fig. 7b-c. It is found that the as-obtained ZnO are 3D hierarchical nanoflowers which are built up by nanoflakes. The morphologies are similar to the case of the precursor. Therefore, the calcination did not destroy the

CrystEngComm Accepted Manuscript

morphologies of 3D hierarchical flow-like nanostructures.

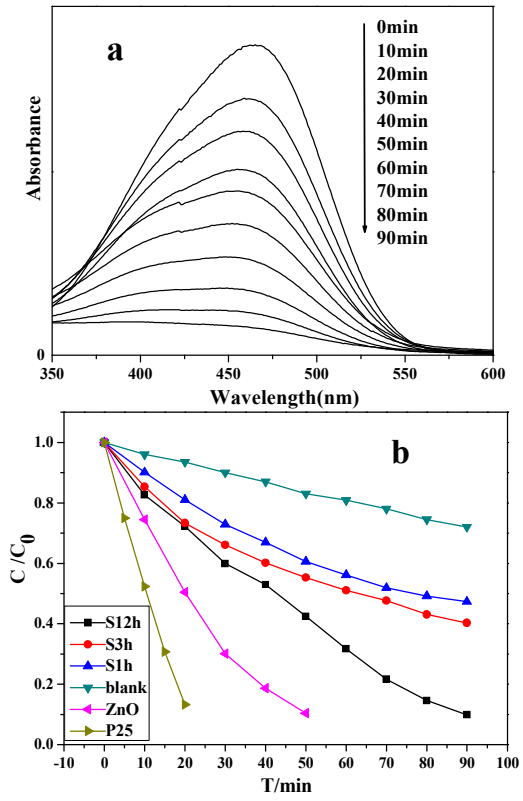

Fig. 8 (a) Absorption spectra of the MO in the presence of hierarchical ZnOHF nanoflowers under UV light and (b) photodegradation efficiencies of MO as a function of irradiation time.

The photocatalytic properties of ZnOHF were investigated by the decomposition of MO under UV light irradiation. Fig. 8a shows the temporal evolution of the absorption spectra during the photocatalytic degradation of MO in the presence of hierarchical flower-like ZnOHF nanostructures. The characteristic absorption of MO at 462 nm was used to monitor the degradation process as a function of irradiation time. With the extension of the exposure time, the absorption peaks are decreased in intensity rapidly and almost disappeared after 80 min. The decrease in absorption was accompanied with a slight shift of the main absorption peak to lower wavelength due to the formation of the demethylated dyes. Fig. 8b shows the photodegradation efficiency of MO as a function of irradiation time. C is the absorption of MO at 462 nm at time T and C_0 is the absorption of MO before irradiation. The degradation of MO was very slow without photocatalyst. While in the presence of the photocatalyst, the intensity of the characteristic adsorption peak decreased dramatically, implying that the hierarchical flower-like ZnOHF nanostructures possessed photocatalytic activity. Therefore, they can be used as photocatalysts to decompose organic compounds in polluted wastewater. It is noticeable that the degradation rates of the ZnOHF obtained from 12 h are higher than that of 1 h or 3 h. It is well known that the size, crystallinity, morphology and surface areas of photocatalyst have important effect on the photocatalytic activity.[25-26] Therefore, compared to S_{3h}, the higher photocatalytic activity of S_{12h} may be attributed to its well crystallinity and larger BET surface area. It is noticeable that the degradation rates of the as-prepared ZnO are higher than that of ZnOHF. ZnO has also been widely studied for photodegradation of pollutants due to its efficacy in degrading various pollutants owing to its high catalytic activity.[27-28] In this study, the as-obtained flower-like ZnO nanostructures show high photocatalytic activity for the degradation of MO.

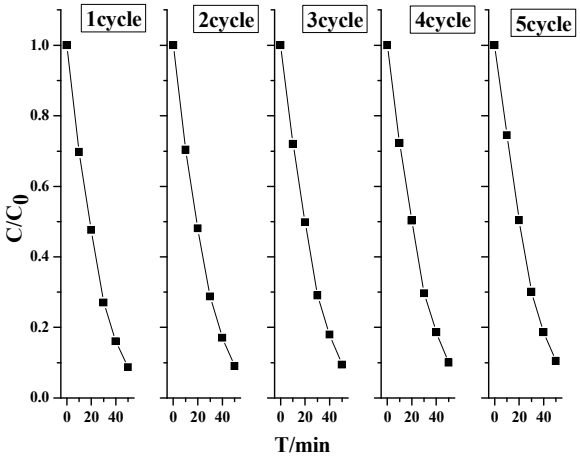

Fig. 9 Cyclability of photocatalytic activity of hierarchical flower-like ZnO nanostructures under UV light irradiation.

Considering the practical application of photocatalysts, the cyclical stability of photocatalyst is of great importance. Fig. 9 shows the cycle tests of hierarchical flower-like ZnO nanostructures under UV light irradiation. The results indicate that the hierarchical ZnO nanoflowers are chemically stable, and the efficiency remained almost the same after five cycles. Therefore, the hierarchical flower-like ZnO nanostructures are promising UV light photocatalyst for practical applications.

Conclusions

3D hierarchical nanoflakes-assembled flower-like ZnOHF nanostructures are synthesized through a one-pot template-free hydrothermal route by using $(NH_4)_2SiF_6$ as fluoride source. The reaction parameters such as the reaction time, temperature and fluoride source play crucial roles in the formation of ZnOHF nanoflowers. 3D hierarchical ZnO nanoflowers are formed by the calcination of ZnOHF in air at 600 °C. The as-prepared ZnO nanoflowers exhibit excellent UV light photocatalytic activity for the degradation of MO, which will endow them potential applications in the treatment of waste water.

Acknowledgments

This work was supported by the National Natural Science Foundation of China (No. 21173122, 21376124) and Natural Science Foundation of Jiangsu Province of China (No. BK2010281).

Notes

CrystEngComm Accepted Manuscript

This journal is © The Royal Society of Chemistry [year]

College of Chemistry and Chemical Engineering, Nantong University, Nantong 226019, P. R. China. E-mail: hi_wangmiao@163.com; Fax: ++86-513 85012851

References

1 G. H. Tian, Y. J. Chen, W. Zhou, K. Pan, C. G. Tian, X. R. Huang and H. G. Fu, *CrystEngComm*, 2011, **13**, 2994-3000.

2 F. F. Tao, C. L. Gao, Z. H. Wen, Q. Wang, J. H. Li and Z. Xu, *J. Solid State Chem*., 2009, **182**,1055-1060.

3 X. J. Sun, J. W. Wang, Y. Xing, Y. Zhao, X. C. Liu, B. Liu and S. Y. Hou, *CrystEngComm*, 2011, **13**, 367-370.

4 M. Wang, Y. J. Shi and G. Q. Jiang, Mater. Res. Bull. 2012, **47**, 18-23.

5 M. Wang, G. Q. Jiang, Y. F. Tang and Y. J. Shi, *CrystEngComm*, 2013, **15**, 1001-1006.

6 U. D. Nazirova, K. M. Akhmerov and P. Tashk, *Dokl Akad Nauk USSR*, 1988, **2**, 40-42.

7 Q. L. Huang, M. Wang, H. X. Zhong, X. T. Chen, Z. L. Xue and X. Z. You. *Cryst. Growth Des*. **2008**, 8, 1412-1417.

8 M. Dai, F. Xua, Y. N. Lu, Y. F. Liu and Y. Xie, *Appl. Surf. Sci*. 2011, **257**, 3586-3591.

9 H. N. Chen, L.Q. Zhu, Q. Hou, W. T. Liang, H. C. Liu and W. P. Li, *J. Mater. Chem*., 2012, **22**, 23344-23347.

10 J. S. Wu and D. F. Xue, *Nanosci. Nanotechnol. Lett*., 2011, **3**, 400-406.

11 J. K. Song, M. B. Zheng, Z. J. Yang, H. Q. Chen, H. Y. Wang, J. S. Liu, G. B. Ji, H. Q. Zhang and J. M. Cao, *Nanoscale Res Lett*., 2009, **4**, 1512-1516.

12 F. Xu, L. T. Sun, M. Dai and Y. N. Lu, *J. Phys. Chem. C*, 2010, **114**, 15377-15382.

13 F. Xu, Y. N. Lu, L. T. Sun and L. J. Zhi, *Chem. Commun*., 2010, **46**, 3191-3193.

14 M. Wang, X. L. Shen, G. Q. Jiang and Y. J. Shi, *Mater. Lett*., 2012, **87**, 54-57.

15 Y. Peng, H. Y. Zhou and Z. H. Wang, *CrystEngComm*, 2012, **14**, 2812-2816.

16 L. Y. Wu, J. B. Lian, G. X. Sun, X. R. Kong and W. J. Zheng. *Eur. J. Inorg. Chem.*, 2009, **20**, 2897-2900.

17 L. J. Zhu, Y. T. Zheng, T. Y. Hao, X. X. Shi, Y. T. Chen and J. Ou-Yang, *Mater. Lett*., 2009, **63**, 2405-2408.

18 M. Wang, T. T. Chen, Y. F. Tang, G. Q. Jiang and Y. J. Shi, *Chin. J. Inorg. Chem.*, 2012, **28**, 185-190.

19 M. Wang, X. L. Shen,Y. F. Tang, G. Q. Jiang and Y. J. Shi, *Chin. J. Inorg. Chem.*, 2012, **28**, 2660-2666.

20 H. X. Zhong, M. Wang, H. L. Yang, J. M. Hong, Q. L. Huang and X. T. Chen, *Mater. Sci. Eng. B*, 2009, **156**, 62-67.

21 N. Saito, H. Haneda, W.S. Seo and K. Koumoto, *Langmuir*, 2001, **17**, 1461-1469

22 S. Yamabi and H. Imai, *J. Mater. Chem*., 2002, **12**, 3773-3778

23 S. Y. Hou, Y. C. Zou, X. C. Liu, X. D. Yu, B. Liu, X. J. Sun and Y. Xing, *CrystEngComm*, 2011, **13**, 835-840.

24 G. H. Tian, Y. J. Chen, W. Zhou, K. Pan, C. G. Tian, Y. Z. Dong, C. G. Tian and H. G. Fu, *J. Mater. Chem.*, 2011, **21**, 887-892.

25 L. Zhang, X. F. Cao, X. T. Chen and Z. L Xue, *J. Colloid Interface Sci*., 2011, **354**, 630-636

26 B. Ohtani, F. Amano, A. Yamakata, K. Nogami and M. Osawa, *J. Am. Chem. Soc*., 2008, **130**, 17650-17651.

27 W. L. Ong, S. Natarajan, B. Kloostra and G. W. Ho, *Nanoscale*, 2013, **5**, 5568-5575.

28 S. Chakrabarti and B. K. Dutta, *J. Hazard. Mater*., 2004, **112**, 269-271.

CrystEngComm Accepted Manuscript